Scenario-based Unit Commitment Optimization for Power System with Large-scale Wind Power Participating in Primary Frequency Regulation

Lili Hao, Jing Ji, Dongliang Xie, Haohao Wang, Wei Li, and Philip Asaah

***Abstract*—Continuous increase of wind power penetration brings high randomness to power system, and also leads to serious shortage of primary frequency regulation (PFR) reserve for power system whose reserve capacity is typically provided by conventional units. Considering large-scale wind power participating in PFR, this paper proposes a unit commitment optimization model with respect to coordination of steady state and transient state. In addition to traditional operation costs, losses of wind farm de-loaded operation, environmental benefits and transient frequency safety costs in high-risk stochastic scenarios are also considered in the model. Besides, the model makes full use of interruptible loads on demand side as one of the PFR reserve sources. A selection method for high-risk scenarios is also proposed to improve the calculation efficiency. Finally, this paper proposes an inner-outer iterative optimization method for the model solution. The method is validated by the New England 10-machine system, and the results show that the optimization model can guarantee both the safety of transient frequency and the economy of system operation.**

***Index Terms*—Unit commitment optimization, primary frequency regulation (PFR), wind power, transient frequency safety, high-risk stochastic scenario, inner-outer iterative optimization.**

I. Introduction

THE total amount of wind power connected to power system increases year by year. In 2017, the global installed capacity of wind power increased by 52492 MW, and the cumulative installed capacity reached 539123 MW, an increase of 11% compared with the end of 2016 (487279 MW) [1]. The grid-integration problems of wind farms have become research hotspots [2]-[4]. Usually, the rotor speed of wind turbine is decoupled from system frequency. Thus, when the system frequency changes, unlike conventional units adjusting the output through governor control or rotating kinetic energy change, the output of wind power generation cannot change with frequency. Such wind power adjustment characteristic may affect the safety of system frequency and the situation will be more serious as wind power capacity increases. Because of the significant uncertainty of wind power, power systems with large-scale wind power penetration need more reserve capacity to ensure the frequency security [5]. However, the reserve capacity generally provided by conventional units decreases due to the decreasing capacity proportion of conventional units, which makes it necessary for wind power generations to participate in PFR. Unit commitment optimization with wind power participating in PFR can provide guarantees for a coordinated operation of conventional units and wind power generations, and make full use of all kinds of sources in power systems.

The start-up, shutdown and power generation costs of conventional units, spinning reserve capacity costs and wind curtailment costs are generally considered in the objective function of the unit commitment model [6]-[8]. The PFR capability of wind power generations is not considered in most of the current studies for unit commitment, and only the randomness of wind power output is considered [6]-[13]. With the consideration of stochastic wind power, the fuzzy mathematical model, the chance-constrained programming and the scenario method are usually used to establish the unit commitment model [6], [7], [9]-[13]. References [12], [13] perform unit commitment optimization in multiple stochastic scenarios to balance the economy and safety of system. Confidence level is usually used as a scenario-selection index to reduce the number of stochastic scenarios, which may ignore low-probability but high-risk scenarios and lead to high risk of system operation. Constraints of power balance, unit output limitation, ramp rate, minimum on/off time, and so on, are generally used by unit commitment. Reference [14] introduces an analytical calculation method for transient frequency security constraints, but it can only be used in the power system where all unit governor-prime movers are identical. In [15], [16], system frequency security constraints are added to the unit commitment model, but the PFR capability of wind power is not considered and only central forecasting scenarios are considered. Both primary and tertiary reserve constraints in the unit commitment model for conventional units are considered in [17], but the impact of wind power access needs to be analyzed further. In brief, the actual PFR

Manuscript received: June 21, 2019; accepted: April 16, 2020. Date of Cross-Check: April 16, 2020. Date of online publication: October 29, 2020.

This work was supported by the Six Talent Peaks Project in Jiangsu Province (No. XNY-020) and the State Key Laboratory of Smart Grid Protection and Control.

L. Hao, J. Ji (corresponding author), and P. Asaah are with the School of Electrical Engineering and Control Science, Nanjing Tech University, Nanjing 211816, China (e-mail: lili_hao@163. com; 708878505@qq. com; asaahphilip@yahoo.com).

D. Xie, H. Wang, and W. Li are with State Grid Electric Power Research Institute, Nanjing 211106, China (e-mail: xiedongliang@sgepri.sgcc.com.cn; wanghaohao@sgepri.sgcc.com.cn; liwei@sgepri.sgcc.com.cn).

DOI: 10.35833/MPCE.2019.000418

capability of the power system is related to its operation scenario, but frequency safety characteristics of the power system in high-risk stochastic scenarios are rarely evaluated in existing literature, and environmental benefits are generally ignored.

Wind power generations can have reserve capacity through de-loaded operation [18]-[20]. Virtual inertia control and droop control should also be added to make wind power generations have the similar PFR function as conventional units [19]-[24]. However, wind power generations are seldom involved in PFR in the unit commitment model, and even if they are used in PFR, the control method is usually very simple. Wind turbines participate in PFR only through the inertia control which provides very limited reserve for system PFR, and only one scenario is considered [25].

The rest of this paper is organized as follows. Section II proposes a unit commitment optimization model considering the coordination of steady state and transient state for power system with large-scale wind power participating in PFR. In the transient-state part, the scenario-selection method based on the ratio of the remaining risk (RR) of PFR to the total remaining risk (TRR) of PFR is further studied. The solution method for the unit commitment model is put forward. Section III tests the abovementioned unit commitment model using the New England 10-machine system. Section IV draws the conclusions.

II. Unit Commitment Optimization with Large-scale Wind Power Participating in PFR

A. Unit Commitment Optimization Model Considering Coordination of Steady State and Transient State

In this paper, a scenario-based unit commitment optimization model considering the coordination of steady state and transient state is built to solve the unit commitment problem for the power system with large-scale wind power participating in PFR. The operation mode of the power system is determined in steady state in the expected scenario of maximum probability, and the transient frequency analysis of the system using the steady-state unit commitment results is performed in transient state in stochastic fluctuation scenarios. The objective function considering the steady-state operation cost C_1 and the transient-state control cost C_2 in stochastic scenarios is built, as shown in (1). Besides the conventional unit start-up cost and the coal consumption cost, the wind power de-loaded cost and the carbon emission cost are added into the steady-state operation cost, in order to reflect the loss of wind farm participating in PFR through de-loaded operation and the environmental benefits, as shown in (2). In this paper, rotor over-speed control is combined with pitch angle control to realize wind generation de-loaded operation, which makes wind power generations give out more PFR power when needed. Equation (3) is the transient-state control cost in high-risk stochastic scenarios including various normal or abnormal disturbances such as one or two devices out of operation, and stochastic fluctuations of load and power supply. The maximum frequency deviation affected by both the inertia and PFR reserve capacity of power system is multiplied by a certain weight as one of the transient-state control costs, which is defined as transient frequency safety cost in this paper. Besides, interruptible loads are adopted in this paper as one of the PFR reserve sources in transient-state process. The cost of wind power curtailment is also considered in the transient-state control costs. Furthermore, wind turbine operation conditions in the same wind farm are supposed to be same, and the power energy cost of units during the PFR process is neglected.

$$\min C = C_1 + C_2 \tag{1}$$

$$C_1 = \sum_{t\in T}\left[\sum_{i\in N^{\mathrm{G}}} y_{i,t}\cdot SUC_{i,t} + \Delta t\left(\sum_{i\in N^{\mathrm{G}}} u_{i,t}C(P_{i,t}) + \sum_{j\in N^{\mathrm{W}}} q^{\mathrm{W}}_{j,t} d_{j,t} P_{j,t}\right) + C^{\mathrm{C}}_t\right] \tag{2}$$

$$C_2 = \sum_{t\in T}\left\{\sum_{s\in S} P_s\left[\Delta t\left(\sum_{k\in N^{\mathrm{IL}}} q^{\mathrm{L}}_{k,t}\cdot IL_{k,t,s} + \sum_{j\in N^{\mathrm{W}}} q^{\mathrm{W}}_{j,t}\cdot WL_{j,t,s}\right) + q^{\mathrm{f}}\left|\Delta f_{\mathrm{nadir},t,s}\right|\right]\right\} \tag{3}$$

$$SUC_{i,t} = \begin{cases} SUC^{\mathrm{hot}}_i & \tilde{T}^{\mathrm{off}}_{i,t} \le T^{\mathrm{cold}}_i + T^{\mathrm{off}}_i \\ SUC^{\mathrm{cold}}_i & \tilde{T}^{\mathrm{off}}_{i,t} > T^{\mathrm{cold}}_i + T^{\mathrm{off}}_i \end{cases} \tag{4}$$

$$C(P_{i,t}) = a_i P^2_{i,t} + b_i P_{i,t} + c_i \tag{5}$$

$$C^{\mathrm{C}}_t = q^{\mathrm{C}}\left(\Delta t \sum_{i\in N^{\mathrm{G}}} u_{i,t}\sigma_i P_{i,t} - vD_t\right) \tag{6}$$

where T is the time series; N^{G} is the conventional unit series; N^{W} is the wind farm series; $y_{i,t}$ is the binary variable that is equal to 1 if unit i is started up in interval t and 0 otherwise; $SUC_{i,t}$ is the start-up cost of conventional unit i in interval t (shutdown cost is approximately zero); $u_{i,t}$ is the binary variable that is equal to 1 if unit i is on in interval t and 0 otherwise; $C(P_{i,t})$ is the output fuel cost of conventional unit i in interval t; $P_{i,t}$ is the power scheduled for conventional unit i in interval t; $d_{j,t}$ is the de-loaded level of wind farm j in interval t; $P_{j,t}$ is the maximum output of wind farm j in interval t; C^{C}_t is the carbon emission cost in interval t; P_s is the probability of scenario s; $q^{\mathrm{L}}_{k,t}$ is the unit electricity price of interruptible load k in interval t; $q^{\mathrm{W}}_{j,t}$ is the unit electricity price of wind farm j in interval t; S is scenario series; N^{IL} is the interruptible load series; $IL_{k,t,s}$ is the load shedding imposed on interruptible load k in interval t of scenario s; $WL_{j,t,s}$ is the amount of wind power curtailment for wind farm j in interval t of scenario s; q^{f} is the weight of maximum frequency deviation; $\Delta f_{\mathrm{nadir},t,s}$ is the maximum frequency deviation in interval t of scenario s; SUC^{hot}_i is the hot start-up cost of unit i; SUC^{cold}_i is the cold start-up cost of unit i; $\tilde{T}^{\mathrm{off}}_{i,t}$ is the off-time of unit i in interval t; T^{off}_i is the off-time limit for unit i; T^{cold}_i is the cold start-up time of unit i; a_i, b_i, c_i are the fuel cost coefficients of conventional unit i; q^{C} is the CO_2 transaction price; σ_i is the carbon emission intensity of conventional unit i; v is the carbon emission benchmark of unit electricity; and D_t is the total power generation of system in interval t, including conventional units and wind farms.

The steady-state constraints include start-up constraint,

output constraint, ramp up and down constraints and minimum on/off time constraint for conventional units. Since the above constraints have been extensively studied in the conventional unit commitment problem, the details are not presented. Other relevant constraints are as follows.

1) Steady-state Constraints

1) System power balance constraints:

System power balance constraints considering the de-loaded operation of wind farms are as follows:

$$\sum_{i\in N^{\mathrm{G}}} u_{i,t}P_{i,t} + \sum_{j\in N^{\mathrm{W}}} \left(1-d_{j,t}\right)P_{j,t} = L_t + D_{Loss,t} \tag{7}$$

where L_t is the load demand of time interval t; and $D_{Loss,t}$ is the line loss of time interval t.

2) Wind farm de-loaded level constraints

The operation characteristics of wind turbines lead to the de-loaded level constraints of wind farm as below.

$$0 \le d_{j,t} \le d_{\max} \tag{8}$$

where $d_{\max}$ is the maximum de-loaded level of wind farm.

3) PFR reserve capacity constraints

Considering the day-ahead forecasting error of wind power and load power, the basic constraints for the PFR reserve capacity of the power system are required, and the reserve sources include conventional units and wind farms. The upper reserve capacity constraints are shown in (9) and (10), and the lower reserve capacity constraints are similar to (9) and (10).

$$P_{i,t}^{\mathrm{f}} = \min\left(P_i^{\max} - P_{i,t}, u_{i,t}\chi_{i,t}\frac{\Delta f_{\max} - D_i^{\mathrm{db}}}{R_i}\right) \tag{9}$$

$$\sum_{i\in N^{\mathrm{G}}} P_{i,t}^{\mathrm{f}} + \sum_{j\in N^{\mathrm{W}}} d_{j,t}P_{j,t} \ge \varepsilon_t \sum_{n\in \Phi^{\mathrm{l}}} L_{n,t} + \sum_{j\in N^{\mathrm{W}}} \xi_{j,t}P_{j,t} \tag{10}$$

where $P_{i,t}^{\mathrm{f}}$ is the total PFR reserve capacity from conventional unit i in interval t; $P_i^{\max}$ is the maximum technical output of conventional unit i; $\chi_{i,t}$ is the binary variable that is equal to 1 if unit i works in the mode that cannot provide primary frequency response in interval t and 0 otherwise; $\Delta f_{\max}$ is the maximum frequency deviation; D_i^{db} is the frequency dead band of unit i; R_i is the frequency regulation constant of conventional unit i; ε_t is the prediction error coefficient of load in interval t; Φ^{l} is system bus series; and $\xi_{j,t}$ is the prediction error coefficient of wind power for wind farm j in interval t.

2) Transient-state Constraints

It is necessary to consider the frequency safety constraints of the power system in transient-state constraints, including maximum frequency deviations, steady-state frequency deviations and initial frequency drop rates. Besides, the constraints for wind power curtailment and interruptible loads in high-risk stochastic scenarios should be considered as well.

1) The security constraints of the transient frequency offset of the power system in stochastic scenarios is as follows:

$$\left|\Delta f_{\mathrm{ss},t,s}\right| \le \left|\Delta f_{\mathrm{nadir},t,s}\right| \le \Delta f_{\max} \tag{11}$$

where $\Delta f_{\mathrm{ss},t,s}$ is the steady-state frequency deviation in interval t of scenario s. Due to the complexity and diversity of the power system, the system frequency obtained by traditional computational analysis methods is generally not very accurate, thus the transient frequency in this paper is mainly obtained by using simulation softwares such as DIGSILENT/PowerFactory.

2) To ensure that the system frequency variation rate is not greater than the limit value in each stochastic scenario, the following constraint is added:

$$\left|RoCoF_{t,s}\right| \le RoCoF_{\max} \tag{12}$$

where $RoCoF_{t,s}$ is the variation rate of frequency in interval t of scenario s; and $RoCoF_{\max}$ is the maximum variation rate of frequency.

3) Interruptible load constraints:

$$0 \le IL_{n,t,s} \le IL_{n,t,s}^{\max} \tag{13}$$

where $IL_{n,t,s}$ and $IL_{n,t,s}^{\max}$ are the amount of interruptible loads at bus n in interval t of scenario s and the maximum amount, respectively.

4) Wind power curtailment constraints of wind farm:

$$0 \le WL_{j,t,s} \le (1-d_{j,t})P_{j,t,s} \tag{14}$$

where $P_{j,t,s}$ is the maximum output of wind farm j in interval t of scenario s.

B. Selection of High-risk Stochastic Scenarios

In order to ensure the safe operation of power system, it is necessary to verify the transient frequency stability of the unit combination results in all possible system scenarios. If the applicability of the result is poor, it needs to be corrected to improve the robustness of the final optimization result. Suppose that each scenario for day-ahead unit commitment includes 24 time intervals which are the same as those of unit commitment, and that each scenario keeps unchanged in each interval. Considering load fluctuations, wind power fluctuations and equipment failures, scenario tree tool (STT) is used to randomly generate multiple disturbance scenarios together with their probabilities, which form the whole scenario set for the day-ahead unit commitment optimization. STT uses the historical wind power, load consumption and fault data as inputs. Monte Carlo simulation is used to generate the required set of scenario trees.

Considering multiple kinds of disturbance in power system, the number of stochastic scenarios is huge. Fortunately, among massive disturbance scenarios, only part of those high-risk scenarios will trigger the revision of unit commitment results. In order to improve the calculation efficiency, a new scenario-selection method which can keep both high-probability scenarios and low-probability but high-risk scenarios is built to form an optimization scenario set in this paper. The ratio of the RR of PFR in each scenario to the TRR of PFR in the whole scenario set is built as the key basis for scenario select to preserve high-risk scenarios. RR is defined as the scenario occurrence probability multiplied by the power deficit (or surplus) outside the safe range of PFR reserve of power system in this scenario. The threshold of RR is set as a proportion of TRR. TRR is defined as the sum of RRs of all scenarios, and its threshold can be pre-set according to the security requirement of system operation. From an initial empty set, the specific steps to determine a reasonable optimization scenario set is as follows:

Step 1: based on the optimized unit commitment results of the previous iteration, TRR is calculated.

Step 2: if the TRR is less than its pre-set threshold, the process of scenario selection ends; otherwise, RRs of scenarios

that have never been selected in any previous iteration are calculated, then the scenarios whose RR values exceed the threshold are selected and set as a scenario subset to be aggregated.

Step 3: the scenarios in the scenario subset to be aggregated are clustered into one scenario which is then added to the optimization scenario set [26], and the probability of each scenario in the optimization scenario set is recalculated.

Step 4: based on the model of Section II-A, the unit commitment result is further optimized in the optimization scenario set, and then return to *Step 1*.

This method can not only preserve high-risk scenarios, but also reduce the scenario number greatly, which can provide a practical way to reduce the risk of system operation. The specific flow chart is shown in Fig. 1, where i is the sequence number of scenario set to be aggregated; k is the single scenario sequence number after aggregation; and $\rho_{sum}(\cdot)$ is the probability summation of the scenario set to be aggregated.

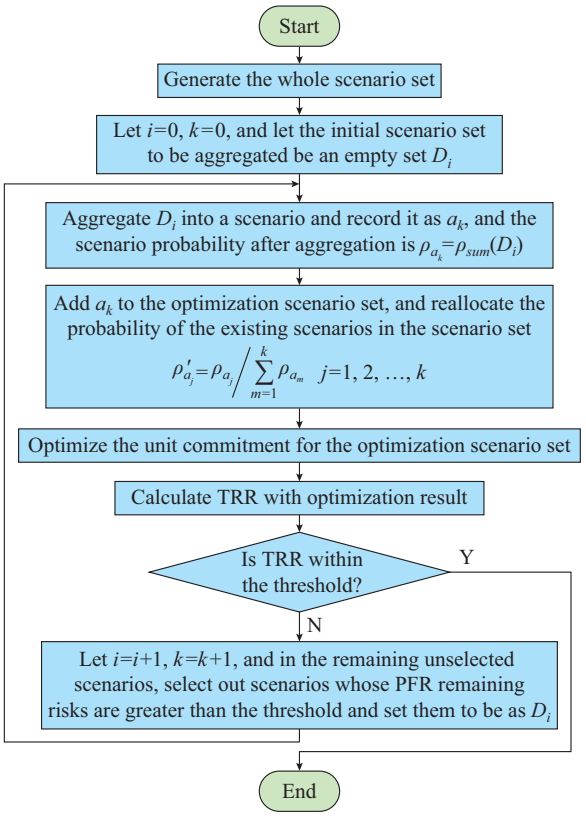

Fig. 1. Scenario-selection process based on ratio of RR of PFR to TRR of PFR.

C. Unit Commitment Solution Based on Inner-outer Iterative Optimization

An inner-outer iterative optimization method for unit commitment is established in this paper, as shown in Fig. 2. In the outer cycle, the optimization scenario set is determined using the method proposed in Section II-B. In the inner cycle, using Benders decomposition method, the unit commitment problem is decomposed into steady-state optimization of unit commitment and transient optimization of interruptible loads and wind power curtailment. The mathematical expressions after the decomposition are as follows.

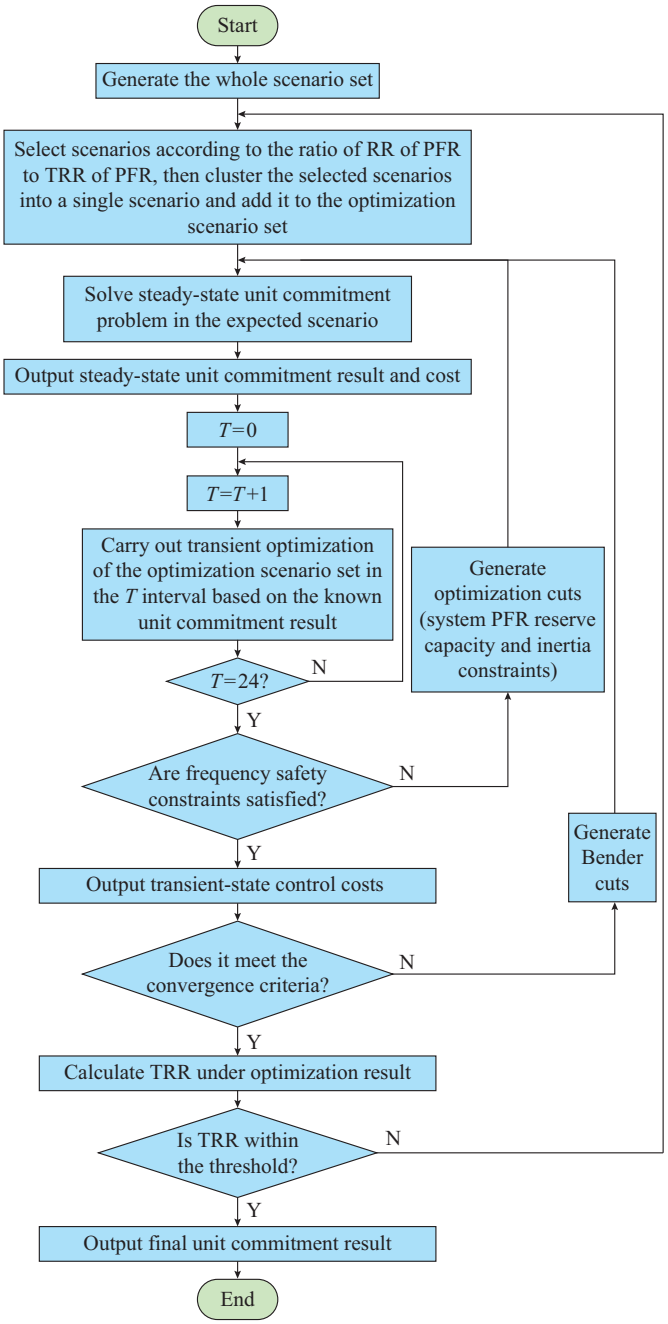

Fig. 2. Solution of unit commitment based on inner-outer iterative optimization.

1) The objective function of the steady-state unit commitment optimization is shown in (15), and the constraints include (7)-(10) and other related steady-state constraints.

$$\min\left\{\omega^{*}+\sum_{t=t_0}^{T}\left[\sum_{i\in N^{G}}y_{i,t}\cdot SUC_{i,t}+\Delta t\left(\sum_{i\in N^{G}}u_{i,t}C(P_{i,t})+\sum_{j\in N^{W}}q_{j,t}^{W}d_{j,t}P_{j,t}\right)+C_t^{C}\right]\right\} \tag{15}$$

where ω^{*} is the Benders cut and corresponds to the mismatch at each cycle of transient optimization problem in Benders decomposition.

2) The objective function of the transient optimization is shown in (16), and the constraints are the same as (13) and (14).

$$\min \sum_{s\in S} P_s \left[\Delta t \left(\sum_{k\in N^{\mathrm{IL}}} q^{\mathrm{L}}_{k,t} \cdot IL_{k,t,s} + \sum_{j\in N^{\mathrm{W}}} q^{\mathrm{W}}_{j,t} \cdot WL_{j,t,s} \right) + q^{\mathrm{f}} \left| \Delta f_{\mathrm{nadir},t,s} \right| \right] \tag{16}$$

In the transient optimization process, since the system frequency in the transient problem cannot be analytically expressed by the unit on-off and output status, it cannot be further optimized through generating Benders cuts. Therefore, when the transient frequency in optimization scenarios does not meet the safety requirements, optimization cuts with practical physical significance are adopted in this paper to further optimize the unit commitment result for system frequency safety. For example, if the frequency characteristics in interval t of scenario s do not meet the security requirements, it indicates that the system has insufficient PFR capability, and it is necessary to increase the PFR reserve capacity and the inertia of power system, as shown in (17) and (18). Also, if the frequency characteristics in interval t of scenario s meet the security requirements, in order to ensure that frequency characteristics will not deteriorate, the constraints of the PFR reserve capability of power system should also be added, as shown in (19) and (20).

$$R^{\mathrm{sum}}_{t,s} + IL^{\max}_{t,s} > \hat{R}^{\mathrm{sum}}_{t,s} + \widehat{IL}^{\max}_{t,s} \tag{17}$$

$$H^{\mathrm{sum}}_{t,s} > \hat{H}^{\mathrm{sum}}_{t,s} \tag{18}$$

$$R^{\mathrm{sum}}_{t,s} + IL^{\max}_{t,s} \geq \hat{R}^{\mathrm{sum}}_{t,s} + \widehat{IL}^{\max}_{t,s} \tag{19}$$

$$H^{\mathrm{sum}}_{t,s} \geq \hat{H}^{\mathrm{sum}}_{t,s} \tag{20}$$

where $R^{\mathrm{sum}}_{t,s}$ is the the total PFR reserve capacity in interval t of scenario s, including the reserve capacity of conventional units and the reserve capacity of wind farms; $IL^{\max}_{t,s}$ is the maximum interruptible load capacity that can be invoked in interval t of scenario s; $H^{\mathrm{sum}}_{t,s}$ is the inertia time parameter in interval t of scenario s, including inertia time constants of conventional units and virtual inertia parameters of wind farms; and symbol $\wedge$ is the index of known variables under the previous iteration result.

Besides, when the power surplus of power system is large, the frequency security can be guaranteed directly by the large-scale wind power curtailment or unit cut-off operation, thus the constraints for the lower PFR reserve capacity are not included.

$$\hat{R}^{\mathrm{sum}}_{t,s} = \sum_{i\in N^{\mathrm{G}}} \hat{P}^{\mathrm{f}}_{i,t} + \sum_{j\in N^{\mathrm{W}}} \hat{d}_{j,t} P_{j,t,s} - \sum_{i\in N^{\mathrm{G}}} \gamma_{i,t,s} \hat{P}^{\mathrm{f}}_{i,t} \tag{21}$$

$$\hat{H}^{\mathrm{sum}}_{t,s} = \sum_{i\in N^{\mathrm{G}}} \hat{u}_{i,t} \frac{S_i}{S_{\mathrm{B}}} H_i + \sum_{j\in N^{\mathrm{W}}} \frac{S_j}{S_{\mathrm{B}}} \hat{H}_{j,t,s} - \sum_{i\in N^{\mathrm{G}}} \gamma_{i,t,s} \frac{S_i}{S_{\mathrm{B}}} H_i \tag{22}$$

where S_i is the rated active power of conventional unit i; S_j is the rated active power of wind farm j; S_{B} is the system-based active power; $\gamma_{i,t,s}$ is the binary variable that is equal to 1 if conventional unit i is unexpectedly stopped in interval t of scenario s and 0 otherwise; H_i is the inertia time constant of conventional unit i; and $H_{j,t,s}$ is the virtual inertia parameter of wind farm j in interval t of scenario s.

In order to meet the economic requirement of power system, Benders cuts shown in (23) are needed to modify the constraints of the steady-state unit commitment problem in the $(m-1)^{\mathrm{th}}$ inner cycle until the convergence criterion $\left|\left(\omega^*_m - \omega^*_{m-1}\right)/\omega^*_{m-1}\right| \leq \zeta$ is satisfied [12], where ζ is the convergence tolerance.

$$\begin{aligned} \omega^* \geq\ & \omega\left(\hat{y}_{i,t,m-1}, \hat{u}_{i,t,m-1}, \hat{P}_{i,t,m-1}, \hat{d}_{j,t,m-1}\right) + \\ & \sum_{i\in N^{\mathrm{G}}} \pi_{i,t,m-1}\left(y_{i,t} - \hat{y}_{i,t,m-1}\right) + \sum_{i\in N^{\mathrm{G}}} \phi_{i,t,m-1}\left(u_{i,t} - \hat{u}_{i,t,m-1}\right) + \\ & \sum_{i\in N^{\mathrm{G}}} \mu_{i,t,m-1}\left(P_{i,t} - \hat{P}_{i,t,m-1}\right) + \sum_{j\in N^{\mathrm{W}}} \vartheta_{j,t,m-1}\left(d_{j,t} - \hat{d}_{j,t,m-1}\right) \end{aligned} \tag{23}$$

$$\begin{cases} y_{i,t} = \hat{y}_{i,t,m-1} \rightarrow \pi_{i,t,m-1} \\ u_{i,t} = \hat{u}_{i,t,m-1} \rightarrow \phi_{i,t,m-1} \\ P_{i,t} = \hat{P}_{i,t,m-1} \rightarrow \mu_{i,t,m-1} \\ d_{j,t} = \hat{d}_{j,t,m-1} \rightarrow \vartheta_{j,t,m-1} \end{cases} \tag{24}$$

where $\hat{y}_{i,t,m-1}$, $\hat{u}_{i,t,m-1}$, $\hat{P}_{i,t,m-1}$, and $\hat{d}_{j,t,m-1}$ are the known values of each dispatching variable obtained by the $(m-1)^{\mathrm{th}}$ inner cycle; and $\pi_{i,t,m-1}$, $\phi_{i,t,m-1}$, $\mu_{i,t,m-1}$, and $\vartheta_{j,t,m-1}$ are the marginal values of each dispatching variable in the steady-state problem, which are calculated from the transient problem in the $(m-1)^{\mathrm{th}}$ inner cycle. In this paper, Benders cuts are functions of scheduling variables such as the unit status, the power generation, and the de-loaded level of wind farm. These cuts are lower estimation of operation cost in each cycle of the transient optimization problem.

The inner-outer iterative optimization steps are as follows.

Step 1: in the expected scenario of day-ahead forecasting, the steady-state unit commitment optimization problem is solved, and then go to *Step 2*. Equation (9) is a non-linear term with minimum function, which can be converted into an equivalent explicit linear form according to [17]. Considering that the treatment of other non-linear terms such as (4) has been extensively studied in the conventional unit commitment, it is not discussed in this paper. Therefore, mixed-integer quadratic programming (MIQP) is used to solve the steady-state unit commitment problem in this paper.

Step 2: the transient frequency analysis of the steady-state unit commitment results obtained in *Step 1* is carried out using the optimization scenario set formed by the outer cycle. That is, the transient optimization for each time interval is performed with (16) as the objective function, and (13) and (14) as the constraint conditions. Due to the complexity and diversity of power system, the system frequency obtained by traditional analytical methods is not always accurate. In order to obtain more accurate and reasonable optimization result, the transient frequency characteristics of power system in (11) and (12) can be obtained by simulation softwares such as DIGSILENT/PowerFactory. If the transient frequency characteristics of power system in any optimization scenario do not satisfy security constraints (11) and (12), the optimization cuts (17)-(20) are formed and used to modify the constraints of the steady-state unit commitment problem in the inner cycle, and then return to *Step 1*. Otherwise, if constraints (11) and (12) are satisfied in all optimization scenarios, the transient-state control cost is obtained, and then proceed to *Step 3*.

Step 3: according to the optimization result obtained in *Step 2*, if the cost convergence criterion is not met, the marginal value of each dispatch variable in steady-state optimization problem will be calculated. Then, Benders cuts are formed and used to modify the constraints of the steady-state unit commitment problem, and return to *Step 1*. Otherwise, the inner cycle unit commitment optimization ends.

III. Simulation Results

The New England 10-machine system shown in Appendix A Fig. A1 is used to verify the proposed model in this paper. The system consists of 6 thermal power units, 1 hydropower unit and 3 wind farms. All units have PFR capability. The maximum active power of thermal power units G1-G6 is 1200 MW, 595 MW, 680 MW, 510 MW, 680 MW and 595 MW, respectively. The maximum active power of hydropower unit G7 is 850 MW. Wind farms G8-G10 are connected to bus 38, 32 and 37, respectively, and the rated power of G8-G10 is 1660 MW, 1300 MW and 1080 MW, respectively. Thus, the wind power penetration rate is about 25%-50%. The rated power of each wind turbine is 2 MW, and the operation condition of each wind turbine in the same wind farm is supposed to be the same. In the simulation, the maximum de-loaded level of wind farm is supposed to be 40%.

A. Selection of High-risk Stochastic Scenarios

100 scenarios are arbitrarily selected from the whole scenario set as examples, then these scenarios are filtered according to the method in Section II-B. As shown in Fig. 3, 10 scenarios whose ratios of RR of PFR to TRR of PFR exceed the threshold (blue line) in single scenario are obtained. The probability p_s of selected high-risk scenario and the power shortage (or surplus) outside the safe range of the PFR reserve capacity of power system under the previous iteration result, i.e., ΔPS_s, are shown in Table I. Taking scenario 14 as an example, the conventional unit G1 has a shutdown at the beginning of the 10th time interval and recovers at the end of the interval. Besides, the load power and the wind power fluctuate greatly during the whole process of the scenario. Although the probability of scenario 14 is the lowest among the selected 10 scenarios, its power shortage (or surplus) of PFR process is the largest, which makes the ratio of RR of scenario 14 to TRR still high, thus it is also selected out. It can be seen that the scenario selection method can avoid the omission of small-probability but high-risk scenarios and effectively control the actual operation risk of power system. For the whole scenario set, through multiple cycles of selecting and clustering of the high-risk stochastic scenarios, the final optimization scenario set including four high-risk stochastic scenarios is obtained.

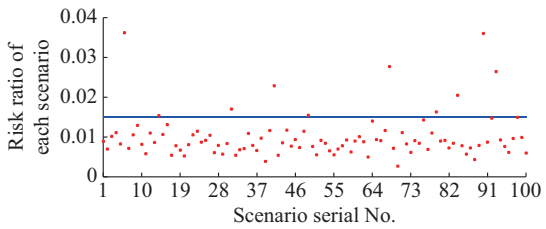

Fig. 3. Scenario selection based on ratio of RR of PFR to TRR of PFR.

TABLE I
Results of p_s and ΔPS_s in Different Scenarios

Scenario serial No.	p_s	ΔPS_s (MW)
6	0.0250	10642
14	0.0083	13604
31	0.0167	7480
41	0.0167	10063
49	0.0167	6796
68	0.0333	6105
79	0.0167	7167
84	0.0167	9009
90	0.0417	6334
93	0.0167	11625

B. Unit Commitment Optimization

The price of interruptible load and the corresponding maximum frequency offset weight are supposed to be 145 $/MWh and $q^f = 1.45 \times 10^5$ $/Hz, respectively. Based on the proposed unit commitment model, the CPLEX software is used to solve the day-ahead unit commitment problem. The results are shown in Fig. 4 and Fig. 5, and the total cost is $8.23 million.

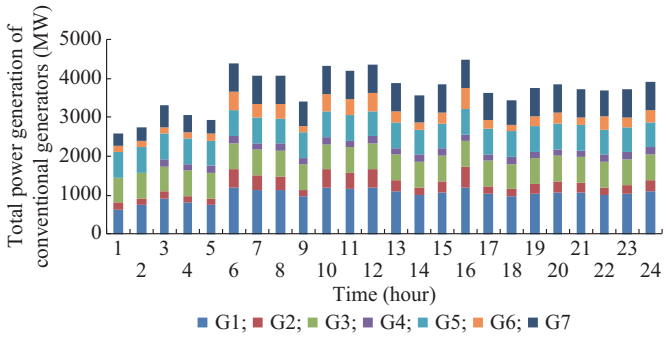

Fig. 4. Output planning for conventional units.

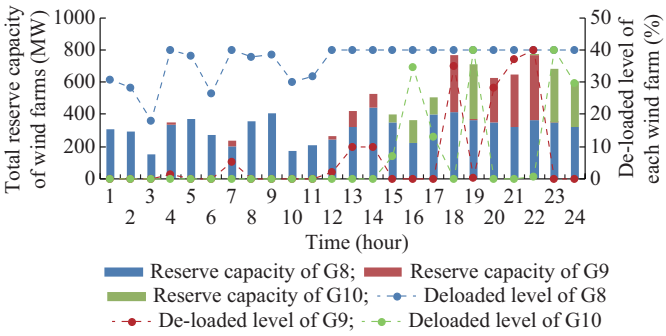

Fig. 5. Wind farm de-loaded levels and steady-state reserve capacity.

From Figs. 4 and 5, the following results can be obtained.

1) Due to the low coal consumption, the output of thermal power units G3 and G5 is not subject to the fluctuation of net load (the difference between load power and wind power), and remains at a high output level during the entire optimization period. On the contrary, the coal consumption of other thermal power units is relatively high, thus their output changes with the fluctuation of net load. Among them, G1

has a higher proportion of total output because of its large capacity. When the net load of power system is small in some intervals, for example, the first two intervals, since the coal consumption of thermal power unit G4 is the largest, it is optimized for shutdown. In that case, the system demand for PFR reserve can be shared by wind farms and other conventional units to improve the economic benefit.

2) Gradually increasing prediction error is added in the experiment to study the influence of scenario prediction on unit commitment optimization. The PFR reserve capacity of wind farms basically increases with the increase of prediction error. With a high penetration of wind power, the total PFR reserve capacity of wind farms is relatively large, which becomes an important source of PFR reserve for power system. In addition, the hydropower unit G7 prepares more PFR reserve capacity than thermal power units because of the larger PFR reserve capacity.

3) The de-loaded priority of wind farm is related to the price of de-loaded wind power. For example, the price of de-loaded wind power of G8 is lower than that of other wind farms, so G8 has priority for de-loaded operation.

In order to compare the influences of different factors in the optimization model, based on the unit commitment model proposed in this paper (model a), three other optimization models are derived from model a, which are as follows:

1) Model b: only the power regulation capacity of interruptible loads in model a is removed.

2) Model c: only the transient frequency safety cost of model a is neglected.

3) Model d: only the PFR function of wind farms in model a is removed.

In the optimization scenario set obtained from Section III-A, due to the uncertainty of large-scale wind power and load power, model d cannot satisfy basic constraints for the PFR reserve capacity of power system. As a result, the interruptible loads will be shed largely, and the economy and safety of power system will be terrible. Hence, the optimization results of other three models in the same scenarios are compared, as shown in Fig. 6 and Appendix A Table AI.

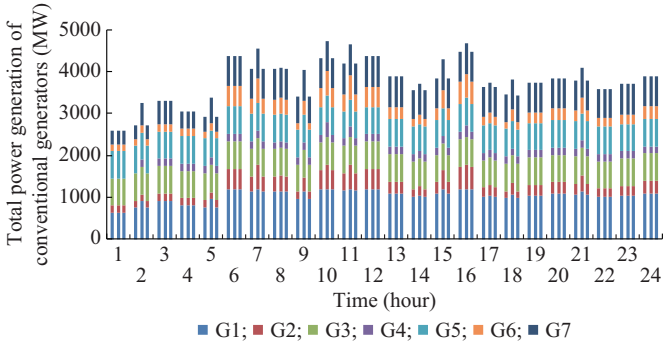

Fig. 6. Output planning for conventional units in different unit commitment models (models a, b and c are presented from left to right in each time interval).

When model b is used, the total output of conventional units during the 2nd, 5th, 7th, 8th, 9th, 10th, 11th, 14th, 15th, 16th, 17th, 18th and 21st time intervals is higher than that of model a. This is because without considering the power regulation capacity of interruptible loads, the PFR reserve capacity of power system and the de-loaded level of wind farms in some extreme cases increase to make system frequency meet the security requirements. The total cost is increased by $0.48 million compared with that of model a. The comparison of the maximum frequency deviations of four optimization scenarios S1-S4 with different unit commitment models is shown in Fig. 7, where S1(a) represents the maximum frequency deviations of scenario S1 with model a, and the rest symbols are defined in analogy.

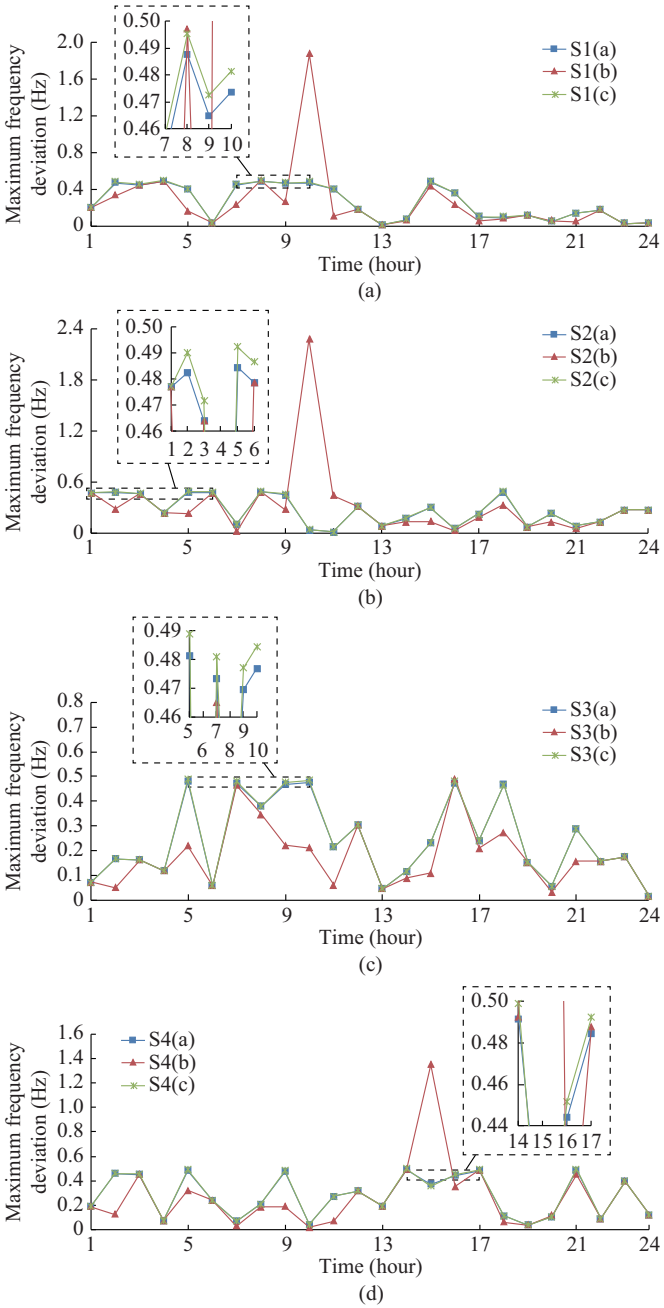

Fig. 7. Comparison of maximum frequency deviations in four optimization scenarios with different unit commitment models. (a) Scenario S1. (b) Scenario S2. (c) Scenario S3. (d) Scenario S4.

At the cost of abandoning economic benefit, although the optimization result of model b under normal disturbances can ensure that the maximum frequency deviations of power

system are lower than those of model a in some time intervals, the system frequency deviations cannot meet the security requirements when severe disturbances occur, such as the 10th interval of scenario S1 (the maximum frequency deviation is 1.8690 Hz), the 10th interval of scenario S2 (the maximum frequency deviation is 2.280 Hz), and the 15th interval of scenario S4 (the maximum frequency deviation is 1.3495 Hz). At the same time, it can be found in Appendix A Table AI that during the 10th and 15th intervals, the de-loaded levels of wind farms all reach the maximum value, and conventional units are all turned on, which makes the system provide its maximum PFR reserve capacity as far as possible. However, the system frequency still cannot meet the security requirements and the frequency over-limit range is very large. It can be seen that in high-risk stochastic scenarios, the participation of interruptible loads in PFR can improve the safety and economy of the overall system operation.

In contrast, frequency security requirements can be satisfied when model c is adopted, and the total output of the conventional units is lower than that of model a in some intervals, thus reducing the operation cost of the system to a certain extent. But in the optimization scenarios, the frequency security of model c is inferior to that of model a in the whole period. For example, in the frequency deviation range of 0.49 Hz to 0.5 Hz, close to frequency limit, the maximum frequency deviation corresponding to model c appears 6 times, while it only appears once with model a. It can be seen that considering the safety cost of system transient frequency, the system frequency characteristics will be better, and that the system frequency can be kept as far as possible from the dangerous boundary to ensure the safe operation of system, especially under severe disturbances.

IV. Conclusion

In addition to conventional units participating in PFR, wind farms are also considered as PFR participants of power system. A scenario-based unit commitment model considering the coordination of steady state and transient state is proposed for unit commitment problem. Interruptible loads and transient frequency offset are also considered in the transient process. The results show that this unit commitment model ensures not only the economic performance of power system operation but also the frequency safety of power system in various high-risk stochastic scenarios.

The ratio of the RR of PFR in the scenario to the TRR of PFR in the whole scenario set is taken as the key basis for scenario selection. Using this method, the number of optimization scenarios decreases significantly, and the omission of low-probability but high-risk scenarios is avoided, so the system operation risk can be effectively controlled within an acceptable range.

Finally, combined with the scenario selection method, a solution method for the unit commitment model is constructed based on the comprehensive consideration of the inertia of power system and PFR reserve demand.

This paper assumes that the operation conditions of wind turbines in the same wind farm are approximately the same, and the situation of multi-type wind turbines in the same wind farm needs further study.

Appendix A

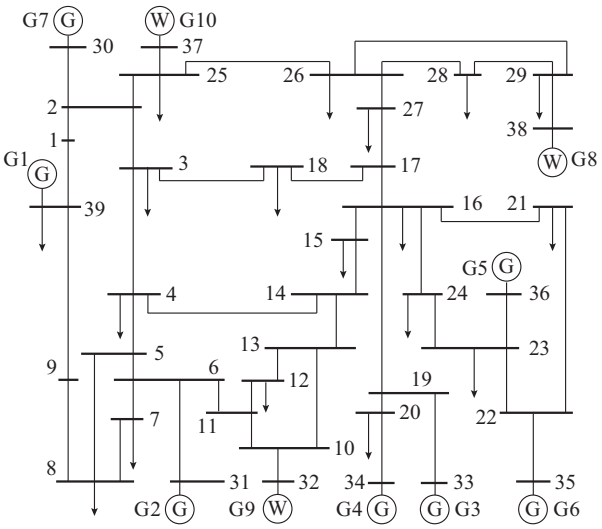

Fig. A1. Diagram of New England 10-machine simulation system.

TABLE AI
Wind Farm De-loaded Levels in Different Unit Commitment Models

Time (hour)	De-loaded level (model a) (%)			De-loaded level (model b) (%)			De-loaded level (model c) (%)		
	G8	G9	G10	G8	G9	G10	G8	G9	G10
1	30.7	0	0	30.7	0	0	30.7	0	0
2	28.2	0	0	40.0	15.20	40.0	28.2	0	0
3	17.9	0	0	17.9	0	0	17.9	0	0
4	40.0	1.20	0	40.0	1.20	0	40.0	1.20	0
5	38.2	0	0	40.0	17.20	40.0	38.2	0	0
6	26.6	0	0	26.6	0	0	26.6	0	0
7	40.0	5.40	0	40.0	40.00	40.0	40.0	5.40	0
8	37.6	0	0	40.0	2.20	0	37.6	0	0
9	38.5	0	0	40.0	40.00	40.0	38.5	0	0
10	29.9	0	0	40.0	40.00	40.0	29.9	0	0
11	31.9	0	0	40.0	40.00	40.0	31.9	0	0
12	40.0	2.30	0	40.0	2.30	0	40.0	2.30	0
13	40.0	10.00	0	40.0	10.00	0	40.0	10.00	0
14	40.0	9.70	0	40.0	25.30	0	40.0	9.50	0.2
15	40.0	0	7.0	40.0	40.00	40.0	40.0	1.40	5.7
16	40.0	0	34.5	40.0	36.30	0	40.0	0	34.5
17	40.0	0	13.0	34.4	40.00	0	40.0	0	13.0
18	40.0	34.80	0	37.1	40.00	40.0	40.0	0	38.5
19	40.0	0.50	40.0	40.0	0.50	40.0	40.0	0.50	40.0
20	40.0	28.40	0	40.0	9.20	40.0	40.0	28.40	0
21	40.0	36.90	0	40.0	40.00	40.0	40.0	36.90	0
22	40.0	40.00	0.7	40.0	40.00	0.7	40.0	40.00	0.7
23	40.0	0.08	40.0	40.0	0.08	40.0	40.0	0.08	40.0
24	40.0	0	29.6	40.0	0	29.6	40.0	0	29.6
Total cost ($)	8230000			8710000			8220000		

References

[1] G. Bandoc, R. Pravalie, C. Patriche *et al*., "Spatial assessment of wind power potential at global scale: a geographical approach," *Journal of Cleaner Production*, vol. 200, pp. 1065-1086, Nov. 2018.

[2] J. Zou, X. Lai, and N. Wang, "Study on control of pumped storage units for frequency regulation in power systems integrated with large-scale wind power generation," *Proceedings of the CSEE*, vol. 37, no. 2, pp. 564-571, Jan. 2017
[3] L. Zhang, T. Ye, Y. Xin *et al*., "Problems and measures of power grid accommodating large scale wind power," *Proceedings of the CSEE*, vol. 30, no. 25, pp. 1-9, Sept. 2010.
[4] J. Liu, W. Yao, J. Wen *et al*., "Prospect of technology for large-scale wind farm participating into power grid frequency regulation," *Power System Technology*, vol. 38, no. 3, pp. 638-646, Mar. 2014.
[5] A. Khazali and M. Kalantar, "Spinning reserve quantification by a stochastic-probabilistic scheme for smart power systems with high wind penetration," *Energy Conversion and Management*, vol. 96, pp. 242-257, May 2015.
[6] Y. Zhang, J. Wang, B. Zeng *et al*., "Chance-constrained two-stage unit commitment under uncertain load and wind power output using bilinear Benders decomposition," *IEEE Transactions on Power Systems*, vol. 32, no. 5, pp. 3637-3647, Sept. 2017.
[7] X. Ai, X. Han, J. Wen *et al*., "Robust unit commitment considering wind power ramp events," *Transactions of China Electrotechnical Society*, vol. 30, no. 24, pp. 188-195, Dec. 2015.
[8] J. Hetzer, D. Yu, and K. Bhattarai, "An economic dispatch model incorporating wind power," *IEEE Transactions on Energy Conversion*, vol. 23, no. 2, pp. 603-611, Jun. 2008.
[9] J. Yin and D. Zhao, "Fuzzy stochastic unit commitment model with wind power and demand response under conditional value-at-risk assessment," *Energies*, vol. 11, no. 2, pp. 341-348, Feb. 2018.
[10] Y. Wang, S. Zhao, Z. Zhou *et al*., "Risk adjustable day ahead unit commitment with wind power based on chance constrained goal programming," *IEEE Transactions on Sustainable Energy*, vol. 8, no. 2, pp. 530-541, Apr. 2017.
[11] P. Xiong and P. Jirutitijaroen, "Two-stage adjustable robust optimisation for unit commitment under uncertainty," *IET Generation, Transmission & Distribution*, vol. 8, no. 3, pp. 573-582, Mar. 2014.
[12] E. Nasrolahpour and H. Ghasemi, "A stochastic security constrained unit commitment model for reconfigurable networks with high wind power penetration," *Electric Power Systems Research*, vol. 121, pp. 341-350, Apr. 2015.
[13] A. Tuohy, P. Meibom, E. Denny *et al*., "Unit commitment for systems with significant wind penetration," *IEEE Transactions on Power Systems*, vol. 24, no. 2, pp. 592-601, May 2009.
[14] H. Ahmadi and H. Ghasemi, "Security-constrained unit commitment with linearized system frequency limit constraints," *IEEE Transactions on Power Systems*, vol. 29, no. 4, pp. 1536-1545, Jul. 2014.
[15] A. Safari and H. Shahsavari, "Frequency-constrained unit commitment problem with considering dynamic ramp rate limits in the presence of wind power generation," *Neural Computing and Applications*, vol. 31, pp. 5241-5254, Feb. 2018.
[16] Y. Wen, W. Li, G. Huang *et al*., "Frequency dynamics constrained unit commitment with battery energy storage," *IEEE Transactions on Power Systems*, vol. 31, no. 6, pp. 5115-5125, Nov. 2016.
[17] J. F. Restrepo and F. D. Galiana, "Unit commitment with primary frequency regulation constraints," *IEEE Transactions on Power Systems*, vol. 20, no. 4, pp. 1836-1842, Nov. 2005.
[18] J. Li, Y. Ma, G. Mu *et al*., "Optimal configuration of energy storage system coordinating wind turbine to participate power system primary frequency regulation," *Energies*, vol. 11, no. 6, pp. 1396-1411, May 2018.
[19] Y. Fu, Y. Wang, X. Zhang *et al*., "Analysis and integrated control of inertia and primary frequency regulation for variable speed wind turbines," *Proceedings of the CSEE*, vol. 34, no. 27, pp. 4706-4716, Sept. 2014.
[20] G. Zhang, J. Yang, F. Sun *et al*., "Primary frequency regulation strategy of dfig based on virtual inertia and frequency droop control," *Transactions of China Electrotechnical Society*, vol. 32, no. 22, pp. 225-232, Nov. 2017.
[21] Y. Chen, G. Wang, Q. Shi *et al*., "A new coordinated virtual inertia control strategy for wind farms," *Automation of Electric Power Systems*, vol. 39, no. 5, pp. 27-33, Mar. 2015.
[22] A. Teninge, C. Jecu, D. Roye *et al*., "Contribution to frequency control through wind turbine inertial energy storage," *IET Renewable Power Generation*, vol. 3, no. 3, pp. 358-370, Sept. 2009.
[23] P. K. Keung, P. Li, H. Banakar *et al*., "Kinetic energy of wind-turbine generators for system frequency support," *IEEE Transactions on Power Systems*, vol. 24, no. 1, pp. 279-287, Feb. 2009.
[24] K. V. Vidyanandan and N. Senroy, "Primary frequency regulation by deloaded wind turbines using variable droop," *IEEE Transactions on Power Systems*, vol. 28, no. 2, pp. 837-846, May 2013.
[25] T. Lin, J. Ye, S. Li *et al*., "Dynamic frequency-constrained unit commitment in isolated grids with DFIGs for frequency regulation," *Journal of Renewable & Sustainable Energy*, vol. 9, no. 5, pp. 559-607, Sept. 2017.
[26] J. Dupacova, N. Growe-Kuska, and W. Romisch, "Scenario reduction in stochastic programming: an approach using probability metrics," *Mathematical Programming*, vol. 95, no. 3, pp. 493-511, May 2003.

Lili Hao received the B.S. and M.S. degrees from Hohai University, Nanjing, China, in 2001 and 2004, respectively, and the Ph. D. degree from Southeast University, Nanjing, China, in 2010, all in electrical engineering. She was a Visiting Scholar in the school of Electrical Engineering and Computer Science, Washington State University, Pullman, USA, from 2015 to 2016. She is currently an Assistant Professor at Nanjing Tech University, Nanjing, China. Her current research interests include power system security and reliability.

Jing Ji received the B.S. degree from Nanjing Tech University, Nanjing, China, in 2017, where she is currently pursuing the M.S. degree in Nanjing Tech University. Her current research interests include wind power generation and smart grid systems.

Dongliang Xie received the M.S. degree from Royal Institute of Technology (KTH), Stockholm, Sweden, and the Ph.D. degree in electrical engineering from Southeast University, Nanjing, China, in 2012. During 2011-2012, he was a Research Associate in Hong Kong Polytechnic University, Hong Kong, China. He is currently working for State Grid Electric Power Research Institute, Nanjing, China. His research interests include analysis, simulation and control for smart grid architectures and essentials consisting of renewable power generation, power market and power system interactions, and demand elasticity.

Haohao Wang received the B.S. degree from Hohai University, Nanjing, China, in 2001, and the Ph.D. degree from Southeast University, Nanjing, China, in 2007, all in electrical engineering. He is currently a Professorate Senior Engineer of State Grid Electric Power Research Institute, Nanjing, China. His current research interests include power system security and reliability.

Wei Li received the B.S. and M.S. degrees from Harbin Institute of Technology, Harbin, China, in 1998 and 2000, respectively, and the Ph. D. degree from Zhejiang University, Hangzhou, China, in 2003, all in electrical engineering. He was a Postdoctoral Researcher in the School of Electrical Engineering, Virginia Tech University, Blacksburg, USA, from 2007 to 2008. He is currently a Professorate Senior Engineer of State Grid Electric Power Research Institute, Nanjing, China. His current research interests include power system security and reliability.

Philip Asaah received the Higher National Diploma (HND) from Sunyani Polytechnic, Sunyani, Ghana, in 2006, in electrical and electronic engineering. He has been working in Ghana Broadcasting Corporation, Ghana, as a Technician Engineer since 2009 to date. Currently, he is pursuing the M.S. degree in Nanjing Tech University, Nanjing, China. His research interests include wind/solar power generation, smart grid systems and control science.